Energy & Environmental Science

A Phytophotonic Approach to Enhanced Photosynthesis

Journal:	*Energy & Environmental Science*
Manuscript ID	EE-PER-09-2020-002960.R2
Article Type:	Perspective
Date Submitted by the Author:	03-Nov-2020
Complete List of Authors:	Kunz, Larissa; Stanford University, Chemical Engineering Redekop, Petra; Carnegie Institute for Plant Biology Ort, Donald; University of Illinois at Urbana-Champaign, Carl R. Woese Institute for Genomic Biology; United States Department of Agriculture, Photosynthetic Research Unit Grossman, Arthur; Carnegie Institute for Plant Biology Cargnello, Matteo; Stanford University, Chemical Engineering Majumdar, Arun; Stanford University, Mechanical Engineering

A *Phytophotonic* Approach to Enhanced Photosynthesis

Larissa Y. Kunz,[a] Petra Redekop,[b] Donald R. Ort,[c] Arthur Grossman,[b] Matteo Cargnello,[a] Arun Majumdar[d]

[a] Department of Chemical Engineering, Stanford University
[b] Carnegie Institution for Science, Department of Plant Biology
[c] Departments of Crop Sciences and Plant Biology, University of Illinois at Urbana Champaign
[d] Departments of Mechanical Engineering and Photon Science and Precourt Institute for Energy, Stanford University

Abstract

Photosynthesis is the dominant biotic carbon sink on earth and hence presents an opportunity for enhanced sequestration of CO_2. If the average net carbon fixation efficiency of terrestrial plants could be increased by 3.3%, all anthropogenic CO_2 accumulating in the atmosphere could instead be reduced and incorporated into terrestrial biomass. Plants make inefficient use of the overly abundant sunlight available to them, a result of having evolved to be competitive and survive highly dynamic environmental conditions rather than maximize photosynthetic productivity. We explore herein a *phytophotonic* approach to enhanced photosynthesis, whereby sunlight is redistributed by means of luminescent or persistent luminescent (PersL) materials. Phytophotonics has potential at varied scales, ranging from photobioreactors to greenhouses all the way to crops in the field, the latter having the potential to impact planetary CO_2 levels. The approach is three-fold: a spectral redistribution to relieve high-light-stress at the top surface of leaves and increasingly drive photosynthesis deeper in leaves and canopies; a minute-scale temporal redistribution to bridge periods of intermittent shade and reduce shock associated with variable light conditions; and a multiple-hour temporal redistribution to shift a fraction of high-intensity midday lighting to evening hours. Based on simulations of photoluminescent materials and light quality experiments with a model algal system, it is shown that while lengthening daylight hours will require significant improvements in PersL materials, the other two approaches show more immediate promise. We demonstrate a means of concentrating PersL light from $SrAl_2O_4$:Eu,Dy, approaching levels needed to effectively bridge periods of natural shade, and outline the scientific questions and technical hurdles remaining to realize the benefits of the proposed spectral shift.

Broader Context

Agriculture represents humankind's first foray into geoengineering. We have a significant impact on the terrestrial biosphere, with food production taking up about 40% of earth's land surface. Since terrestrial photosynthesis plays a major role in the carbon cycle, agricultural practices have the potential to significantly impact the carbon balance—both as an emitter and as a carbon sink, via biosequestration. However, since the end of the Green Revolution, further improvements to plant growth efficiencies (especially crop yields) have become progressively more difficult to realize. To this end, plant and agricultural scientists are increasingly looking for novel and interdisciplinary methods of increasing photosynthetic efficiencies.

Introduction

Despite the accelerating growth of research and development of sustainable energy technologies, climate models predict that these technologies, influenced by the global political, economic, and social climate, will be insufficient to cap rising temperatures at 2°C through the reduction of CO_2 emissions. To combat climate change, technologies for negative emissions must be developed to complement sustainable energy practices. With atmospheric levels slightly over 400 ppm CO_2, though, direct carbon capture from air unfortunately remains prohibitively expensive based on the inverse power law scaling of separation cost with concentration.[1] However, *bio*sequestration already takes place on a massive scale, with terrestrial biomass taking up about 120GT-carbon/year and oceans taking up about 90GT-carbon/year, most of which is reduced and converted into organic carbon molecules through photosynthetic processes.[2]

Since almost 10% of that terrestrial biosequestration is attributed to agricultural carbon fluxes,[3-6] the carbon fixation efficiency of croplands significantly influences the planetary carbon cycle. Not only is improved agricultural efficiency desirable for the carbon budget, but improved crop yields are also needed to meet the food production demands of a growing population and accommodate improving standards of living. The UN Food and Agriculture Organization estimates that a 70% increase in food production will be needed by 2050 (based on 2005 production levels).[7]

Unfortunately, photosynthesis is inefficient at capturing solar energy into plant biomass. As shown in Figure 1, of the solar energy incident on a plant, 51% is lost due to being outside the photosynthetically active spectrum, and 5% is lost due to reflection and transmission. Of the absorbed 44% that can hypothetically be used for photosynthesis, 20% is lost by the photosystems due to inherent thermodynamic limits, 10-15% is lost during carbohydrate biosynthesis, and up to 8% is lost to photorespiration (in C3 plants) and mitochondrial respiration. However, under high light intensity conditions experienced for much of the day, <10% of the absorbed photons can actually be used for photosynthesis due to light saturation of sunlight leaf photosynthesis, drastically cutting the overall efficiency.[8] Despite the resulting <1% net energy efficiency of carbon fixation in most plants,[9] a mere 3.3% *relative* increase (e.g., from 1% to 1.033%, calculation in the SI) in the net carbon fixation efficiency of terrestrial plants would result in the fixation of all anthropogenically generated CO_2 that is currently accumulating in the atmosphere at a rate of 3-4 GT-carbon/year.

State-of-the-art

The development of agriculture represents the first, albeit unintentional, human experiment in geoengineering. Centuries of conventional tilling methods have led to soil erosion 1-2 orders of magnitude faster than soil production, with soil erosion tracking well with the rise and fall of human civilizations.[10] Today, almost 40% of the earth's landmass is covered in agricultural land.[11] Historically, technological developments have enabled enormous improvements in the yields of croplands (comprising ~30% of the total agricultural land): the green revolution saw widespread application of selective plant breeding, coupled with the application of nitrogen fertilizers, improved irrigation, and pesticides, resulting in massive crop intensification that included a yield per hectare increase from 1960 to 2000 of 208% for wheat, 157% for maize, and 109% for rice.[12] Key genetic improvements underlying this intensification were the production of higher yield varieties followed by the reduction of time needed to reach maturity.[12] This intensification tripled cereal crop production[12] and contributed up to a quarter of the 50% increase in seasonal global atmospheric CO_2 fluctuations—highlighting the potential to manipulate CO_2 levels by altering agricultural practices.[13]

More recently, direct attempts to increase photosynthetic efficiency (rather than crop yields) comprise an active area of research but have limited applications in the field thus far. Most research efforts have focused on improving the activity and selectivity of enzymes in the Calvin-Benson-Bassham (CBB) cycle—especially the carboxylation enzyme Rubisco, improving the mesophyll conductance and concentration of CO_2 in C3 plants, and modifying the photorespiratory pathway to reduce its energetic costs.[14] Targeted manipulations of enzymes participating in the CBB cycle have demonstrated increases in CO_2 fixation rates up to over 30% and increases in biomass up to 60% in controlled growth environments.[15] Recently, the introduction of an alternative photorespiratory pathway in tobacco resulted in 20% increases in photosynthetic quantum yield in the field.[16] Other targeted manipulations of photorespiration, electron transport, and carbon transport have been reported to increase dry weight by up to 50%, 72%, and 71%, respectively, in controlled growth environments and greenhouses, with reduced benefits in field experiments. Modifications to the photosystems have also been proposed, including decreasing antenna size by decreasing chlorophyll content,[17] which may enable reallocation of antenna nitrogen to promote carboxylation and electron transport.[18] While these approaches show promise, single or even

multigene manipulations to photosynthetic processes may not be sufficient, at least in the near term, to adequately increase yields.[15]

As such, alternative approaches to enhancing photosynthetic efficiency should be considered in parallel, including modifying the growing environment to optimally use existing photosynthetic capability. Light availability is a factor that has received less attention, given that it exists above saturation thresholds for much of the growing season. However, while the available energy in incoming solar irradiation is seldom limiting, the temporal, spectral, and spatial distributions of that sunlight within crop canopies are not necessarily optimal for maximal carbon fixation and high yields. Certainly, seasonal variation in CO_2 levels on the Keeling curve[19] suggest that longer daylight and increased light availability contribute to increased carbon fixation on a global scale. Consistent with this observation, longer photoperiods are known to frequently increase plant dry weight, though the specific effects can vary significantly among plant types.[20]

Limited work has been done on redistributing light—temporally, spectrally, or spatially—and has been focused primarily on greenhouses. Photoperiods, light intensities, and spatial light distribution can be tuned in greenhouses to maximize productivity of different crops; many plants demonstrate higher yields with a lengthened photoperiod (up to ~20 hrs) at reduced light intensity.[21, 22] Genetic modifications to confer continuous light tolerance have also been shown to increase tomato yields up to 20%.[23] Another exigent proposal is to use chlorophyll d or chlorophyll f (with red-shifted absorption relative to chlorophyll a and chlorophyll b) to extend photosynthetic activity into the near IR, but this has not yet been achieved.[24] Solar greenhouses have increased in popularity in recent years, using transparent photovoltaics to leverage excess solar energy for power generation; the electricity is used to power the greenhouse, which can include indoor grow lights. A handful of studies have been performed on the use of fluorescent materials to increase the availability of red light; however, the scope of these studies is limited, and experiments were all performed at either low (compared to typical solar) or unspecified light intensities.[25-28] Recently, down-converting (green-to-orange) fluorescent plastic sheeting has become commercially available to retro-fit greenhouses (developed by UbiQD Inc.), but the detailed effects of this spectral conversion have not yet been studied.[29] Overall, despite the potential benefits of light manipulation on photosynthetic efficiency, relatively little work has been done in this space so far.

The Phytophotonic Approach

A phytophotonic approach to increasing carbon fixation focuses on modulating the delivery of light into the system. The approach is two-fold, aiming to increase: (a) the <10% usage of absorbed photons;[8] as well as (b) the availability of light to leaves deeper in the canopy that can be heavily shaded. The idea is to achieve this redistribution of light by means of a passive lighting system, using fluorescent and/or persistent luminescent (PersL) materials to redistribute photons spectrally and/or temporally. As shown in Figure 2, a luminescent material embedded in a stabilizing matrix is suspended over plants, emitting photoluminescent (PL) photons to the adaxial leaf surfaces, but can also be used as a ground cover, emitting PL photons towards the abaxial leaf surfaces.

To provide a sense of what this might look like practically, a few potential implementations of such a PL lighting system are listed below; the potential for realization on these varied scales in important for the expansion potential of such a phytophotonic technology.

(a) Application to photobioreactors, e.g., for algae growth: PersL/PL films might be coated onto photobioreactor outer walls to increase the efficiency of these systems, which can operate on narrow margins.[30-33]
(b) Application to greenhouses: PersL/PL materials might be integrated directly into greenhouse covering materials, including small-scale hoop house covers, to increase crop yields.
(c) Application to outdoor crops: PersL/PL materials might be directly distributed on croplands. The optics of light delivery are likely to be much more complicated outdoors, and such a direct application to plants also raises a host of questions about biological compatibility and environmental impact. As such, this large-scale application, which is needed to have a significant effect on the global carbon balance, is only potentially relevant down the road.

In the following sections, we outline the details of both a spectral and temporal shift in lighting, including: (a) the rationale supporting each approach; (b) the desired target lighting conditions; and (c) the technical limitations in reaching these lighting conditions using currently commercially available materials, especially related to low luminescent intensities. Thereafter, we demonstrate an engineering solution to increase luminescent intensity and provide an outlook on opportunities and remaining challenges in realizing such a phytophotonic approach.

Luminescent materials to redistribute light spectrally

(a) Rationale

The spectral breakdown of irradiation significantly impacts net photosynthetic activity. Red light has long been known to have the greatest action of photosynthetically active radiation (PAR) wavelengths when measured for individual leaves at low light intensities.[34-37] Absorption of red and blue wavelengths is high whereas absorption of green light is low.[35] At light intensities far below stress levels (~100-250 μmol/m^2/s for common higher plants), red and blue light can be fully absorbed near the surface of individual leaves and drive photosynthesis efficiently—in contrast to the weakly absorbed green light.

However, more recent work using higher light intensities and optical thicknesses has indicated that on a system level (i.e., for entire plants rather than individual leaves), green wavelengths, which penetrate deeper into leaves and canopies, may actually contribute significantly.[38-40] In fact, as shown for a spinach leaf in Figure 3, carbon fixation rates—which map very closely to the concentration of the carboxylation enzyme Rubisco[38]—reach their peak in the middle of the palisade mesophyll,[41] where overall light intensities are low and highly enriched in green wavelengths.[42] Under high intensity lighting conditions, the top of a leaf absorbs the red and blue light[35, 39, 43, 44] and becomes saturated, activating non-photochemical quenching (NPQ) responses.[41] The remaining, green-enriched light that penetrates deeper into the leaf, where Rubisco concentrations are higher, is locally below saturation levels and hence will not activate NPQ responses as strongly. This greater penetration depth, combined with sieve and diffusion effects that increase the optical path length of green light, results in relatively high green light absorptance on a system-level.[39] Extending this logic to entire canopies, despite the fact that light saturation conditions nominally prevail for much of the day at the top of the canopy, up to 50% of carbon in plants is actually fixed under light-limiting rather than enzyme-limiting conditions.[45] It has been proposed that this spectral dependence enables a dynamic response to changing light conditions, whereby surface activity (driven mostly by red and blue wavelengths) is high at low light intensities, and deep activity (driven by green wavelengths) is dominant at high light intensities.[38, 39]

(b) Target lighting conditions

Due to the spectral dependence of light intensity profiles with depth, intuiting the optimal emission spectrum of a luminescent lighting system a priori is nontrivial. As qualitative guiding principles, though, we can say that red and blue wavelengths are clearly preferred at low light intensities, supported by a wealth of research over the past 50 years, whereas green wavelengths tend to be more advantageous at high light intensities. To experimentally evaluate the impact of incorporating phytophotonic approaches on the productivity of photosynthetic organisms, we have been using the unicellular green alga *Chlamydomonas reinhardtii*.

Wild type *C. reinhardtii* were grown in photoautotrophic conditions as a model system to determine the impact of green light on net photosynthetic activity. Since the algae are grown in a dispersion that is continuously being shaken, chlorophyll and enzyme depth profiles will not be maintained as they are in the structures of vascular plants; analogously, the extent of photosynthesis and NPQ depth profiles will depend on the shaking speed. However, if the hypothesis that green light significantly drives photosynthesis at greater depths is true, algae grown under green-enriched lighting should be able to grow to higher optical densities. *C. reinhardtii* samples were grown under three lighting conditions, shown in Figure 4a: high intensity white LED lighting (300 μmol/m^2/s, past saturation for this system), 20% reduced intensity white LED lighting (240 μmol/m^2/s), and high intensity lighting enriched in green light (240 μmol/m^2/s white LED light plus 60 μmol/m^2/s 525 nm light). White light intensity was changed stepwise between night and day to reduce stress introduced by the change in intensity. As shown in Figure 4b, the green-enriched lighting promoted an increase in cell counts relative to samples grown under white lighting. A mixed effects ANOVA analysis was conducted on these cell count data from day 6, accounting for variation induced by the lighting conditions (three groups) and variation caused by biological replicates (six biological replicates per group); four repeat cell count measurements were conducted for each biological replicate. The null hypotheses tested were that the green-enriched lighting samples had the same mean cell counts as (a) the high white light samples and (b) the reduced white light samples. These null hypotheses were rejected with p-values of 5.6% and 0.2%, respectively, indicating that the green-enriched lighting had a high probability of positively impacting the growth.

This outperformance was observed over the course of the entire growth period (see Figure S1). The growth profiles correspond to an average reduction in doubling time of 8% and 25% relative to the strong white and reduced light, distinct with mixed effects ANOVA p-values of 8% and 0.2%, respectively (see Figure S1). Here the null hypotheses were that the doubling times were identical between the green-enriched lighting samples and the two white light control groups. Meanwhile, in a control experiment (data not shown), growing algae under high white LED light (270 μmol/m^2/s) and under high white light (270 μmol/m^2/s) plus minimal green light (525 nm, <5 μmol/m^2/s) LED lighting, no significant difference was observed in the final optical density.

Spectral lighting profiles used and photographs of a subset of the samples at the end of the 9-day growth period are included in Figure S1. Chlorophyll a/b ratios were found to be approximately the same across all samples at the end of the growth period (2.5 – 2.6), though transient chlorophyll profiles before acclimation to the varied lighting conditions could be different; the F_v/F_m (i.e., the quantum yield of photosystem II, PSII) was likewise found to be comparable between all samples, within the error of the measurement. (The relatively low F_v/F_m values between 0.4 and 0.5 can be attributed to the combined stressors of minimal growth media, relatively high light, and a diurnal cycle for this *C. reinhardtii* CC124 strain.[46-48]) Full experimental methods are included in the SI.

These systems are complicated, however, and spectral modifications could trigger or interfere with various signaling responses,[49-51] and in vascular plants would include but not be limited to effects on seedling establishment, stem growth, nastic movements, root curvature, flowering, and vegetable growth.[52] Future studies are needed to evaluate the mechanistic effects of such spectral modifications—especially when applied to vascular plants. Of particular interest will be mechanistic studies on the effects of green-enriched high intensity lighting.

(c) Achievability with currently available materials

Based on work in the optoelectronics, spectroscopy, and imaging communities, multitudes of fluorescent organic dyes and inorganic fluorescent nanoparticles exist.[53, 54] Fluorescent dyes report quantum yields approaching 100% in some cases, though the fluorescence efficiency depends on the chemical environment (solvent, surrounding polymer matrix, etc.).[55] Candidate fluorescent nanoparticles that are free of heavy metals include Mn:ZnS, ZnO, and graphene quantum dots, all with emission bands in the ~500-590 nm range and quantum yields over 50%.[56] Inorganic

nanoparticles, especially quantum dots, typically offer the advantages of high quantum yields, broad absorption bands, and readily tunable emission peak widths.[54]

For implementation of such a spectral conversion, green-emitting quantum-dot-embedded polymer films need to be optimized. Aggregation of quantum dots needs to be suppressed to ensure efficient fluorescence, which can be accomplished using techniques reported in the literature; for instance, to embed quantum dots in a polymer matrix in a segregated manner, elevated-temperature, rapid oligomerization can be used to confine isolated quantum dots prior to complete polymerization.[57] To optimize for high transmission and high downward fluorescence through a film suspended above a plant, the quantum dot density must be maximized while minimizing parasitic absorption from the polymer matrix, minimizing film thickness (~10 μm or smaller, depending on the absorption cross-section and density of the quantum dots), and maintaining separation of the quantum dots. If used as a groundcover, illuminating the abaxial sides of leaves, slightly thicker films are actually preferred. Thicker films increase net upwards rather than downwards fluorescence. Note that abaxial illumination drives photosynthesis with lower quantum yields.[39] Red wavelengths might be preferred for low-intensity fluorescent abaxial illumination, even under high intensity adaxial illumination.

Persistent luminescent materials to redistribute light temporally

Temporal light redistribution might be used to address two different effects, namely: (a) smoothing over shock induced by sudden shade (on the time scale of seconds to minutes); and (b) shifting photons from high intensity midday hours to evening or night time hours (on the time scale of hours), thereby increasing illumination hours.

I. To smooth over periods of shade

(a) Rationale

Luminescent lifetimes on the timescale of seconds to minutes promise the benefit of smoothing over changes in lighting conditions. Periods of intermittent shade occur throughout the day, due to cloud cover and shading from other leaves and plants. Due to cloud cover, leaves at the top of a canopy can experience rapid changes in photosynthetic photon flux density (PPFD) up to about $\pm$ 1000 μmol/m^2/s. Mid-canopy leaves, which rely primarily on sunflecks to drive photosynthesis,

can regularly experience rapid fluctuations over $\pm$ 1500 μmol/m^2/s, depending on wind and the structure of the canopy above.[58]

Under the high light intensity of full sun, protective NPQ mechanisms are active, dissipating excess energy contained within excited pigments as heat. These NPQ mechanisms can persist for multiple minutes past the onset of shade, reducing photosynthetic rates and ultimately decreasing carbon assimilation by 20% or even more. Work done on reducing this loss includes genetic manipulations to accelerate the shade response (time it takes for relaxation of quenching) in tobacco plants, which have been shown to increase dry weight by 15%.[59] The transition from shade back to sun then suffers a second set of inefficiencies due to reactivation of photosynthetic machinery. Wheat, for instance, has been shown to require about 15 minutes to recover maximum photosynthetic efficiency after being transferred from shade to sun—a slow response driven primarily by the activation of Rubisco and secondarily by the opening of stomata; this slow recovery has been shown to reduce the net assimilation by as much as 21%.[60]

(b) Target lighting conditions

The kinetics of photosynthetic responses to variable light conditions have been well characterized for many systems. While predicting optimal lighting conditions is plant- and location-specific and remains difficult, guidelines can be outlined based on the existing understanding:

(1) The timescales of activation/deactivation of NPQ, Rubisco, and stomatal conductance are seconds to ~1 minute, ~10 minutes, and ~10 minutes, respectively.[58] As such, persistent luminescence on the order of seconds to minutes may already be useful in fully bridging brief periods of shade.

(2) Luminescent intensity must be sufficiently bright to drive photosynthesis, $\gtrsim$ 1 W/m^2 (5 μmol/m^2/s). A gradual decay in luminescent intensity over a few minutes is preferred, to smooth the transition from full sun to shade and back.

(3) Self-shading (of the lower canopy by the upper canopy) can be significant and highly variable in wind, so intracanopy light distribution is of interest.

To provide further guidance on desirable lighting conditions, we performed preliminary experiments on the impact of low-level (~20 μmol/m^2/s) continuous green lighting combined with

fluctuating white light, again with the unicellular green alga *Chlamydomonas reinhardtii*. Green light was chosen since the most efficient PersL materials to date emit green light. Samples of wild type *C. reinhardtii* were grown in photoautotrophic conditions under variable lighting conditions, including: (a) 16 hr/day high-level white LED lighting (at intensities that saturate photosynthesis in the algae, 300 μmol/m^2/s); (b) 16 hr/day 23%-reduced intensity (240 μmol/m^2/s) white LED lighting; and (c) 16 hr/day 23%-reduced intensity (240 μmol/m^2/s) white LED lighting combined with 16 hr/day low-level green LED lighting (525 nm, 15, 20, and 25 μmol/m^2/s for three different samples). Note that for (c) the maximum light intensity was 260 μmol/m^2/s, lower than the 300 μmol/m^2/s used in (a) and thereby simulating a sub-unity luminescence efficiency. Spectral light profiles are shown in Figure S2a. Light shock (to mimic shade) was introduced via seven 10-minute periods throughout the day during which the white LED lighting was turned off. These lighting profiles are shown in Figure 5a.

After 12 days, cell counts were observed to be marginally elevated in the samples under higher green light (Figure 5b). A mixed effects ANOVA analysis was conducted on these cell count data from day 12, with three lighting condition groups, three biological replicates for each group, and four repeat cell count measurements for each biological replicate. The null hypothesis was that the samples grown under the mixed white (with simulated shading) and green lighting had the same mean cell counts as the low white light samples with simulated shading. This was found to have a p-value of 7.4%. (Meanwhile the control null hypothesis that the high white samples with simulated shading were identical to the low white light samples with simulated shading was accepted with a p-value of 96%). Corresponding doubling times are included in Figure S2, but further study is needed to better quantify this difference. Chlorophyll profiles (Figure S2) and PSII activity (data not shown) were observed to be comparable (within error) across all samples.

(c) Achievability with currently available materials

Strontium aluminate-based oxides with various dopants are well-known PersL materials with particularly high quantum yields, tunable absorption/emission spectra and tunable decay times.[61] Decay times can be tuned to match typical durations needed to bridge periods of shade. Likewise, absorption and emission spectra can be tuned to optimize for maximum increase in biomass yield,

balancing any wavelength-dependent signaling independent of photosynthetic processes[49, 50] with wavelength-dependent, system-level photosynthetic efficiencies.

The absorption and emission spectra of strontium aluminate can be tuned by means of varying the crystal structure[62] and doping with various metals.[63] Resulting emission spectra peak anywhere from UV to red, with quantum yields up to about 90% at room temperature.[64, 65] Monoclinic $SrAl_2O_4$:Eu,Dy, a commonly used persistent phosphor, with a persistence time on the order of hours and a high quantum yield, is the most promising material currently available.[66, 67] Its absorption and emission spectra are shown in Figure 6a. While variants of this material with surface coatings that down-convert the emission are commercially available, their emissions are much less bright.

Unfortunately, despite its high quantum yield, $SrAl_2O_4$:Eu,Dy is insufficiently bright on its own. While afterglow indeed persists for many hours after charging, the emission intensity drops two orders of magnitude within minutes of charging, as shown in Figure 6b for the brightest commercially available samples of $SrAl_2O_4$:Eu,Dy (from GloTech International). Other commercial samples undergo this same drop in intensity within seconds. Under direct sunlight, a film of $SrAl_2O_4$:Eu,Dy embedded in a poly(methyl methacrylate) matrix can emit up to ~5 W/m^2 (~20 μmol/m^2/s); within seconds to minutes of being placed in the dark, however, the luminescent intensity drops to ~0.01 W/m^2 (~0.05 μmol/m^2/s). Since the minimum light intensity needed to drive photosynthesis is ~1 W/m^2 (~5 μmol/m^2/s), the emission intensity needs to be increased by about two orders of magnitude to be useful in smoothing over light fluctuations.

While most high quantum yield PersL materials are based on strontium aluminate, recently organic PersL molecules have been developed, capable of luminescing up to the timescale of hours via exciplex emission of charge-separated states, a significant improvement over the timescale of seconds typically achievable by mere phosphorescence. Unfortunately these organic PersL systems still have relatively low quantum yields below 50%, including both immediate fluorescence and the delayed persistent luminescence.[68, 69] Biocompatible, organic PersL systems might offer benefits as luminescent dyes down the road if integrated into the upper epidermis and/or palisade mesophyll of leaves, but even greater improvements in luminescent intensity will be needed for these organic PersL molecules than for the inorganic PersL materials.

II. To increase illumination hours

(a) Rationale

Midday light saturation conditions exist up to well in the arctic circle at the height of summer in the northern hemisphere, and vegetation between the tropics experiences midday light saturation intensity year-round. Figure 7 shows the distribution of light intensity throughout a clear day—beginning at sunrise—at Stanford University (and other locations of equivalent latitude) at the summer solstice. Assuming photosynthetic light compensation at 5 μmol/m^2/s and saturation at 1250 μmol/m^2/s, about 20% of available photons lie above saturation levels for a typical sun plant (about 45% for a typical shade plant, assuming saturation at 750 μmol/m^2/s), and protective quenching responses reduce the efficiency with which absorbed photons can be used, such that <10% of absorbed PAR photons are actually used to drive photosynthesis under these conditions.[8] Meanwhile, longer daylight hours are known to commonly increase the dry weight of plants. Evidence also points to benefits of low intensity long day light treatments over high intensity short day lighting, perhaps a result of the hyperbolic relationship between PPFD and net photosynthetic rate (within the range of useful light intensities).[20]

One means of temporally redistributing light is to use photovoltaics and batteries to then power LEDs. Modern transparent photovoltaics, sometimes used in greenhouse rooves and driven by UV and IR light, achieve up to 10% efficiency.[70] Accounting for battery and LED efficiency, such a setup could present at best about a 5% increase in useful photon availability.

Alternatively, persistent luminescent (PersL) materials might be used to shift a fraction of the incoming sunlight from the high light intensity midday to the evening hours. Best-case scenarios of this shifted distribution are shown in Figure 7 as well, for persistent luminescent covers that re-emit UV and photosynthetically active radiation (PAR) photons as PAR with 2 hr, 5.5 hr, and 11 hr characteristic decay times. In a photobioreactor or greenhouse, this redistribution might be achieved by integrating a PersL material into the photobioreactor walls or greenhouse roof, respectively. Later down the road, further innovation could enable direct application of solid PersL materials to leaf surfaces and/or transgenic integration of luminescent dyes into the upper epidermis and/or palisade mesophyll of leaves, where light intensity is highest, more readily

expanding application to outdoor crops. Past work on using PersL nanoparticles as biomarkers (for imaging and sensors) might prove useful to this end.[71]

(b) Target lighting conditions

The ideal PersL lighting system would re-emit absorbed photons with 100% quantum efficiency towards the plants, in which case any temporal delay in emission is all upside. This ideal increase in useful photons over the course of the day corresponds to the integrated PPFD from Figure 7 between the minimum to drive photosynthesis and the saturation level and is shown in Figure 8a, assuming all UV and visible wavelengths are absorbed and re-emitted in the visible range. This result sets the upper bound on the potential increase in useful photon availability over the course of a day (for a sun plant located at Stanford University) at ~50%.

For a PersL sheet suspended above a plant, however, maximally 50% of luminescent photons will be emitted down towards the plant (unless a dichroic mirror or other means of capturing upwards luminescent photons is implemented). As a result, there is a trade-off between increasing the fraction absorbed by the PersL cover to increase downwards luminescence and maintaining sufficient transmission of incoming PAR wavelengths so as to not lose too many quanta to upwards luminescence. As shown in Figure 8b, an optimum ensues, at which point the cumulative number of usefully available photons is maximized. From a photon-accounting perspective, efficiencies of 50% or lower require that long luminescent lifetimes be achieved to guarantee an increase in photon availability. The second set of calculations in Figure 8a indicate that a lifetime short of ~4 hours actually results in a net decrease in available photons; these calculations are based on the assumption that 30% of PAR is absorbed by the PersL material, with no contribution from the UV. UV-B light is important for signaling high light intensity conditions via the UVR8 receptor,[72] so UV-free lighting might be undesirable.

While these calculations provide some indication of changes that might be anticipated in PAR photon availability, photosynthetic activity ultimately depends nonlinearly on these changes. Likely more significant in driving up net assimilation than increased integral photon availability are (a) the resulting lengthening of periods of low-intensity lighting (given the hyperbolic relationship between PPFD and net photosynthetic rate[20]) and (b) the accompanying reduction in the load on protective quenching processes. Shade plants would be expected to see greater benefits,

given that their photosynthetic rates saturate at lower PPFDs. It is clear, however, that longer PersL lifetimes are preferred, within the limits of diurnal cycle requirements for the plant(s) of interest.

(c) Achievability with currently available materials

The same PersL materials are relevant here as in the previous section, except that long luminescent lifetimes are now particularly important. $SrAl_2O_4$:Eu,Dy is the most viable candidate for meeting these long lifetimes. However, the emission intensity issue discussed in the previous section becomes increasingly problematic over these longer lifetimes: the emission intensity needs to be increased by at least four orders of magnitude to be useful in lengthening daylight hours. The feasibility of accomplishing such an increase is discussed in the next section.

Addressing the light intensity issue: A PersL concentrator

For the cases involving a temporal delay in emission, the limiting factor to this phytophotonic approach to enhancing photosynthesis is the brightness of the PersL materials. $SrAl_2O_4$:Eu,Dy, currently the brightest PersL material available to the best of our knowledge, stores light by means of relatively deep traps below the conduction band, believed to be either oxygen vacancies or traps related to the presence of dysprosium. Excited electrons trapped in these states are gradually either thermally stimulated or tunnel over to europium fluorescent centers for recombination. Many specific mechanisms have been proposed, and consensus and disagreement across these mechanisms have been summarized by Vitola et al.[73] They all tend to agree that the persistent luminescence is a bulk material property. Consistent with this, larger $SrAl_2O_4$:Eu,Dy crystals tend to be brighter than small crystals. The shape of the luminescence decay curve is indicative of a multitude of trap states with various characteristic times for recombination (as can be deduced by exponential analysis). Surface passivation is useful in suppressing recombination via surface states; many commercial products achieve brighter and longer luminescence in the dark with this strategy, effectively converting fluorescence to PersL.

The $SrAl_2O_4$:Eu,Dy from GloTech International characterized in Figure 6 is, to the best of our knowledge, the brightest commercially available material. Based on the decay kinetics measured at 525 nm reported in Figure 6b, over 99% of the traps have lifetimes greater than 1 s. The relatively high emission intensity under illumination is a result of repeated, rapid excitation and fluorescent

recombination. Under illumination, we measured that at most 80% of the emission can be ascribed to delayed luminescence (assuming a cut-off at 1 s), consistent with what is reported in the literature.[74] A reasonably high quantum yield of 65 ± 10% has been reported for $SrAl_2O_4$:Eu,Dy from this same supplier.[74] Long-term outdoor decay kinetics (overnight) of a thin pellet of this same $SrAl_2O_4$:Eu,Dy demonstrate a drop in intensity of about three orders of magnitude over four hours upon nightfall.[75] For comparison, a sample of slightly smaller grains with surface passivation (50 – 75 μm instead of 1 – 2 mm) demonstrated a drop in intensity of about four orders of magnitude over four hours in a fluorimeter (see Figure S3). The high fraction of deep, PersL trap states and relatively high quantum yield indicate that this low intensity issue is primarily a result of low absorbance.

Total absorption and hence emission can be increased by decreasing scattering boundaries and/or increasing the surface area over which light interacts with the sample. The relatively high refractive index, measured to be between 1.65 and 1.66 with the Becke Line Test, explains the high degree of scattering. While scattering boundaries can be reduced by processing $SrAl_2O_4$:Eu,Dy into a glass ceramic, exigent methods of doing so require reducing conditions at high temperatures (1500 °C)[76] and are hence impractical. Increasing the chances for absorption, similar to a luminescent solar concentrator, is notably simpler; hence we demonstrate the effectiveness of this method in concentrating persistent luminescence emission below.

A PersL concentrator was designed (depicted in Figure 9a-b), consisting of pillars of packed $SrAl_2O_4$:Eu,Dy particles embedded in a transparent acrylic matrix. Incoming light scatters repeatedly off these pillars, thereby increasing the net probability for absorption and subsequent luminescent emission. Surface-passivated 50 – 75 μm $SrAl_2O_4$:Eu,Dy particles (purchased from The Avid Colorist) were packed into the laser-cut holes. Prototypes were made with an angle-averaged spacing between columns, w_{avg}, of 3.9 mm (corresponding to x = 1.4 mm, as defined in Figure 9a), a height of 6.4 mm, and multiple column diameters of d = 500 μm, 400 μm, and 200 μm. The optical properties of these concentrators under simulated solar light (PAR intensity 1800 μmol/m^2/s, from a Newport 94021A Class ABB Solar Simulator with xenon lamp) and then in the dark, ~5 s after illumination, are reported in Figure 9c. As expected, transmission increases with smaller column sizes, covering a smaller fraction of the top surface area. An optimum is seen in fluorescent intensity, balancing increased path length of a ray of light through the device with

parasitic absorption by the acrylic. Note that since the typical UV and blue light (which induce luminescence) penetration depths into metal oxides are less than 1 μm,[77] the minimum column diameter is limited by particle size rather than radiative transport.

To determine the optimal PersL configuration, diffuse light travelling through the concentrator was described with a Monte Carlo simulation. Details of this simulation are included in the SI, and evidence of convergence of the simulation with increasing sample size is given in Figure S4. The trends in transmission and fluorescence observed experimentally (Figure 9c) were reproduced with the simulation (Figure 9d). The quantitative disparity between experimentally measured transmission (~45 – 60%) and simulated transmission (~75 – 90%) can be attributed predominantly to the chamfer at the top of the laser-cut holes, significantly increasing scattering and reflection off the top surface. The simulated fractional intensity of luminescence corresponds to the intensity under illumination, which experimentally drops about one order of magnitude in the ~5 s process of transferring the device from illumination to the dark, when the luminescent intensity was then measured. After accounting for this drop in intensity, quantitative agreement between experiment and simulation is good.

Sensitivity analyses of transmission, upwards fluorescence, and downwards fluorescence with the configurational variables w_{avg} (angle-averaged spacing between $SrAl_2O_4$:Eu,Dy columns) and h (device height) are reported in Figures 10a and 10b, respectively, assuming column diameters of 200 μm. The best PersL concentrator prototype in Figure 9c, labelled as "design 1," had an angle-averaged spacing of w_{avg} = 3.9 mm and a height of 6.4 mm and increased luminescent intensity by almost one order of magnitude. The sensitivity analyses suggest that decreasing the spacing and increasing the height can further increase the luminescent intensity up to about one additional order of magnitude. To this end, an improved PersL concentrator, labelled as "design 2," was made with the following geometric parameters: x = 800 μm, w_{avg} = 1.3 mm, d = 400 μm, and h = 12.7 mm (Figure S5). The device was 3D printed (as opposed to laser-cutting the holes) to enable constant hole width over this larger height, which also removed the aforementioned chamfer issue and increased transmission. Simulation of the device predicted about a 3.5-fold improvement over "design 1." As is shown in Figure 10c, a 3-fold improvement was observed experimentally, and a PPFD over 0.1 μmol/m^2/s was maintained for a couple minutes. As such, this design 2 device demonstrates nearly 30x improvement over the bare sample. In terms of further improving upon

this device, it is worth noting that spacing below 2 mm and heights above 20 mm (for 200 μm holes) may be prohibitively difficult to fabricate. Improvements in 3D printing technology may help in this attempt.

These improvements in luminescent intensity can now be compared to the increases needed to realize the goals of lengthening days and/or bridging shade. Meaningfully, smoothing over light fluctuations appears feasible. Only ~2 orders of magnitude improvement in luminescent intensity are required, and the first order of magnitude was already achieved with a preliminary PersL concentrator prototype (see Figure 10c). Simulation indicated that further optimization should yield the second order of magnitude, and the feasibility of using 3D printing to fabricate these devices opens up a host of possible alternative geometries that might further increase PersL concentration.

Lengthening daylight hours, on the other hand, required ~4 orders of magnitude increase in luminescent intensity. Unfortunately, decay kinetics of even the brightest commercially available $SrAl_2O_4$:Eu,Dy, indicating at least three orders of magnitude drop in intensity over four hours, imply that a charging intensity of at least 1000 W/m^2 would be required to reach the minimum 1 W/m^2 intensity after four hours needed to drive photosynthesis. As such, lengthening daylight hours would likely require improved PersL materials with modified luminescent decay kinetics, e.g., by converting some of the deeper electronic traps into shallower traps.

Conclusion and Future Outlook

While selective breeding and genetic modification have long been studied as means of increasing crop productivity, lighting modifications to increase photosynthetic efficiency have been explored much less due to the overabundance of sunlight. Sunlight, though overabundant, is not optimally distributed spatially or temporally for maximum growth, however, seeing as plants have had to adapt to withstand a wide variety of insolation conditions. The phytophotonic approaches explored in this work, of spectrally and/or temporally redistributing available sunlight to enhance photosynthesis, address these inefficiencies. These redistributions might be achieved passively

with luminescent or persistent luminescent (PersL) materials, benefitting from improvements in these materials over the past few decades.

In the context of spectral redistribution, high quantum yield fluorescent quantum dots and means of processing these materials into maximally luminescent films (or alternatively groundcovers) are already known. Given the relatively high quantum yields of green-emitting materials and building on recent developments in understanding the role of green light in driving photosynthesis on a system level, we recommend investigating the potential of green fluorescent quantum dots. The major remaining hurdle is to optimize films of green fluorescent quantum dots for this application, targeting high-light conditions. Scientific questions remain about physiological implications of specific spectral redistributions, but should any physiological or developmental issues arise, these can likely be addressed by biological engineering.

In the context of temporal redistribution, $SrAl_2O_4$:Eu,Dy, the brightest PersL material commercially available today, shows promise in bridging periods of intermittent shade on the order of seconds to minutes. Effective concentration of the persistent luminescence (for sustained intensities over 1 W/m^2) are anticipated to reduce the loss of photosynthetic efficiency due to slow reinduction caused by cloud cover and self-shading. While lengthening daylight hours to shift photons from high-intensity-midday hours to low-intensity-evening hours may offer significant productivity benefits, an "active" lighting system (e.g., involving photovoltaics and LEDs, as can already be done in greenhouses) is needed, as even concentrated persistent luminescence from $SrAl_2O_4$:Eu,Dy will be insufficient to maintain photosynthetic lighting intensities over four hours.

The network of photosynthetic machinery and its interaction with other metabolic and protective mechanisms are complex, and the effect of any redistribution in light availability cannot be reliably quantitatively predicted at this point. With the multiple phytophotonic approaches explored in this perspective, we outline where we see potential promise and which key scientific questions and technical developments remain to realize such approaches.

Acknowledgements

L.Y. K. acknowledges support from a Stanford Graduate Fellowship (SGF). M. C. acknowledges support from the School of Engineering at Stanford University and from a Terman Faculty

Fellowship. Part of this work was performed at the Stanford Nano Shared Facilities (SNSF), supported by the National Science Foundation under award ECCS-1542152. Thank you also to Sam Bullock for prototyping assistance during the COVID-19 pandemic.

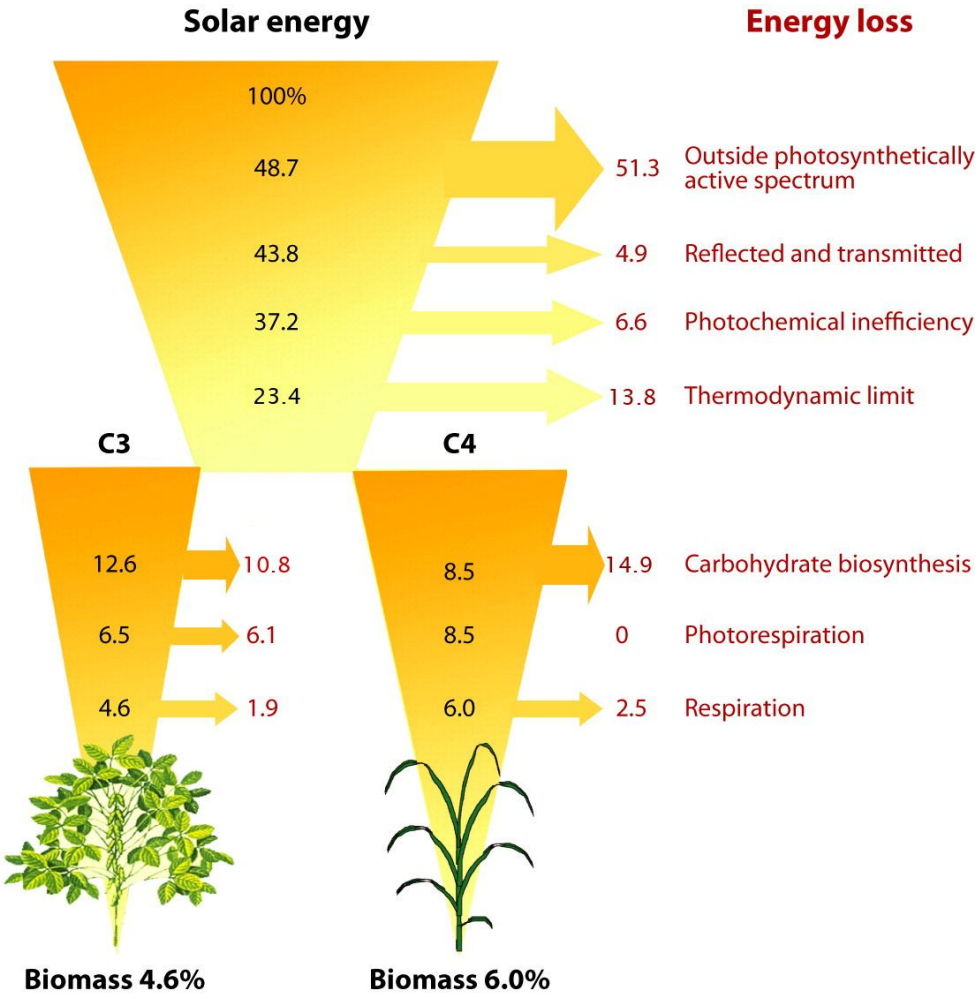

Figure 1. Delineation of minimum energy losses in C3 and C4 plant carbon fixation. Actual efficiencies are much lower, partly due to high light intensity reducing the fraction of absorbed photons that can actually be used for photosynthesis but up to over 90%. Reproduced from reference [8].[8]

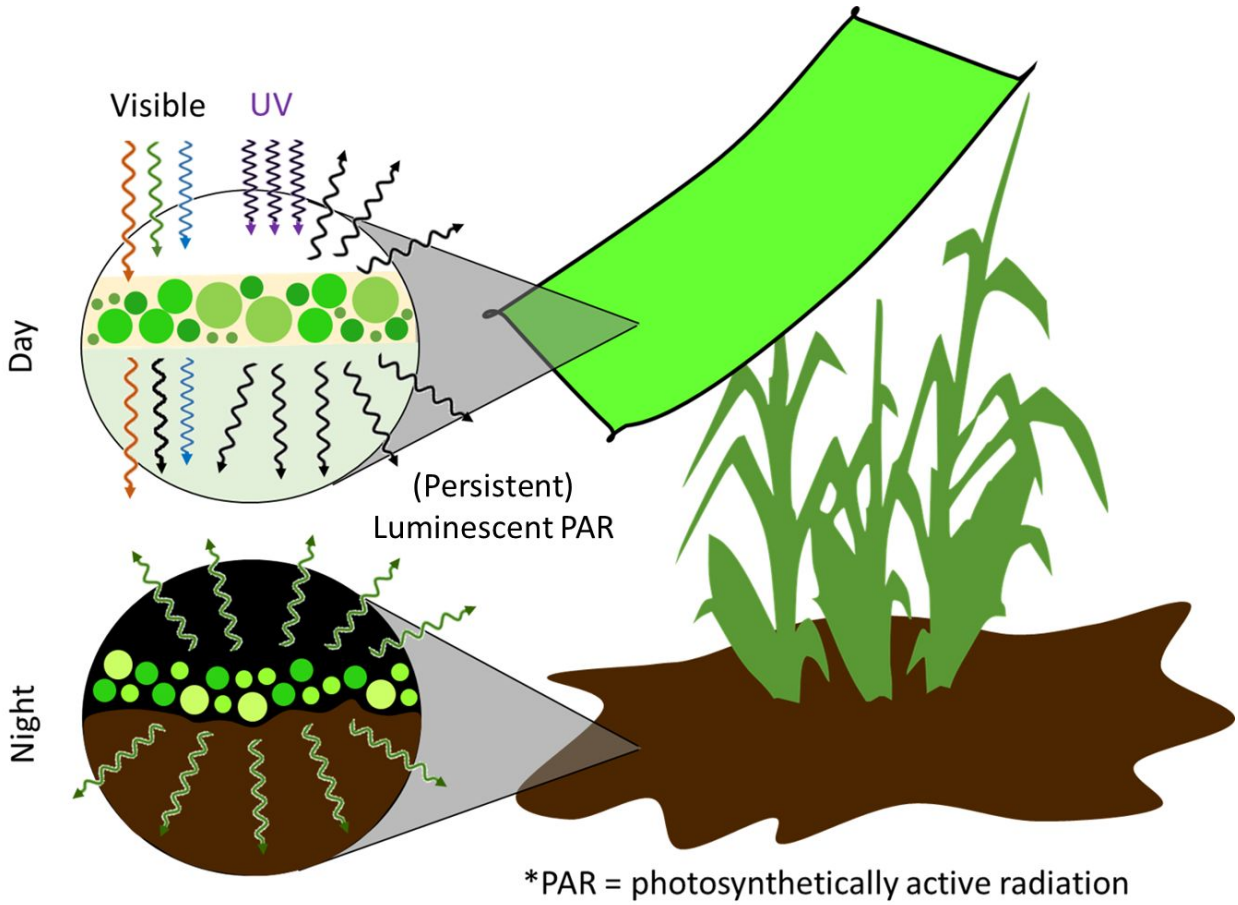

Figure 2. Schematic of the phytophotonic approach, showing a (persistent) luminescent film suspended above a plant or as ground cover.

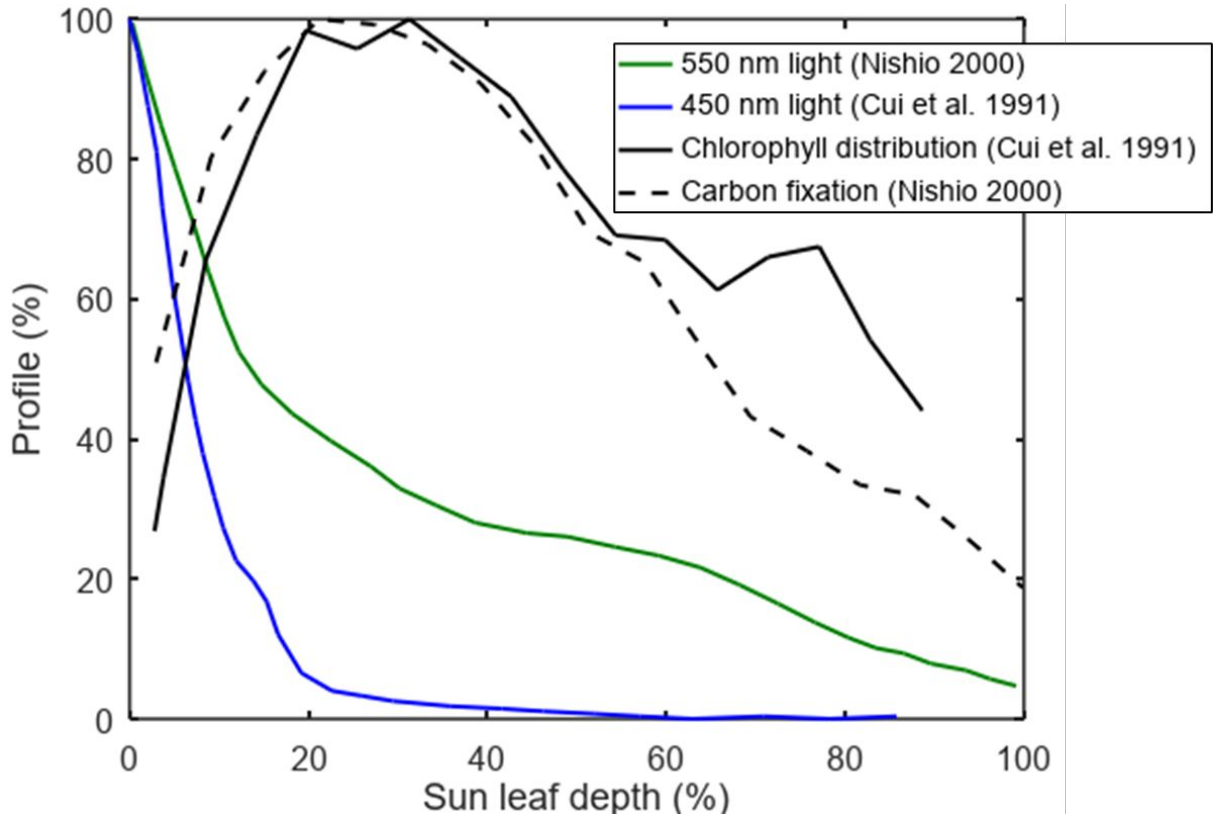

Figure 3. Depth profiles of light absorption, chlorophyll distribution, and carbon fixation through a spinach sun leaf, reproduced from data extracted from Cui et al. 1991 and Nishio 2000. Note that the light intensity profile of red light (not shown here) closely tracks that of blue light, with only a marginally larger penetration depth.[38, 42]

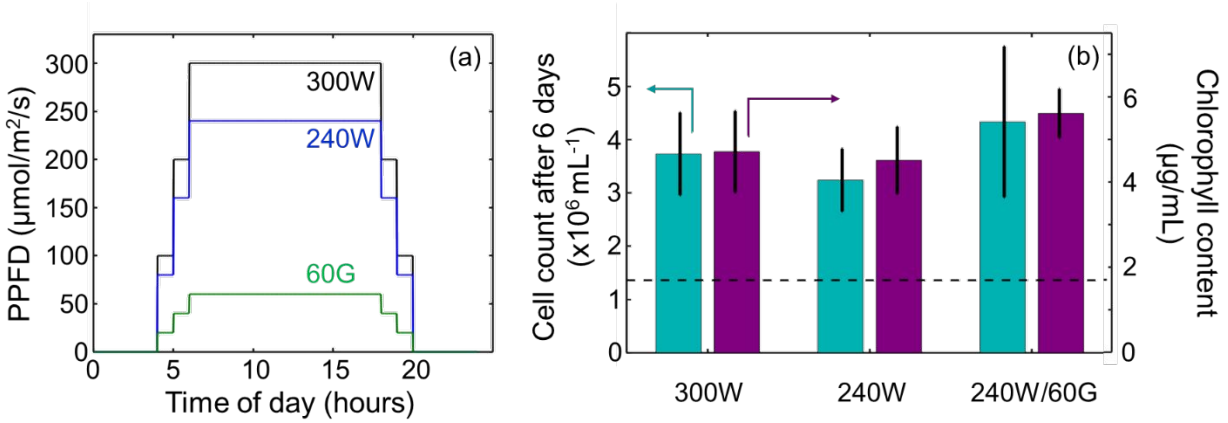

Figure 4. (a) Lighting profiles (measured as photosynthetic photon flux densities, PPFD) used in experiments on the benefits of supplemental green-enriched lighting at high light intensities. 300W refers to 300 μmol/m^2/s white LED lighting; 240W refers to 240 μmol/m^2/s white LED lighting; and 60G refers to 60 μmol/m^2/s green (525 nm) LED lighting. (b) Cell counts (teal, left axis) and chlorophyll concentrations (purple, right axis) of *C. reinhardtii* samples grown under this set of lighting conditions for 6 days, with six biological replicates for each group on day 6. The dotted line indicates the initial cell count at day 0.

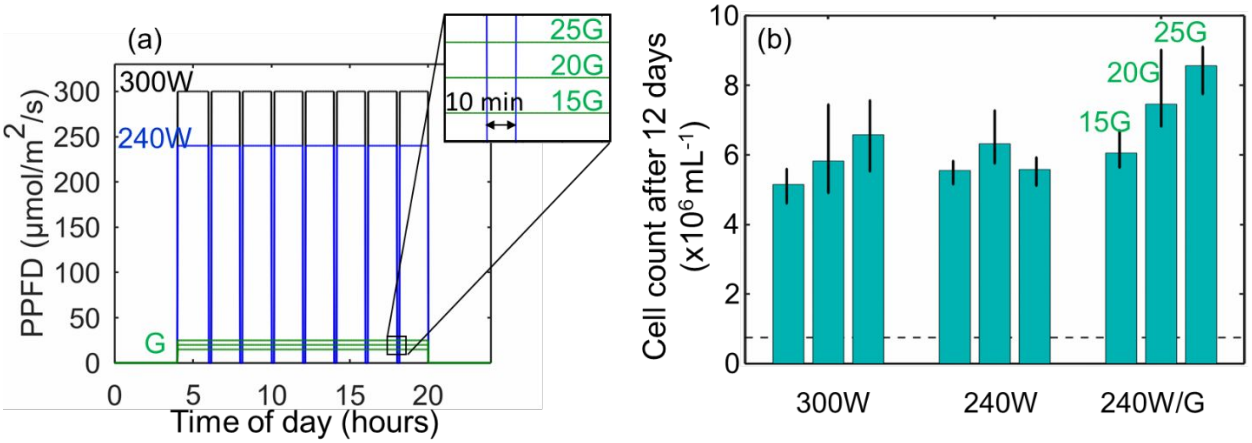

Figure 5. (a) Lighting profiles (measured as photosynthetic photon flux densities, PPFD) used in experiments mimicking intermittent light shock from changing light conditions. 300W refers to 300 μmol/m^2/s white LED lighting; 240W refers to 240 μmol/m^2/s white LED lighting; and 15G/20G/25G refer to 15/20/25 μmol/m^2/s green (525 nm) LED lighting. (b) Cell counts of *C. reinhardtii* samples growing under this set of lighting conditions for 12 days, with error bars indicating minimum and maximum measurements of four repeat cell count measurements and three biological replicate samples for each sample on day 12. The dotted line indicates the initial cell count at day 0.

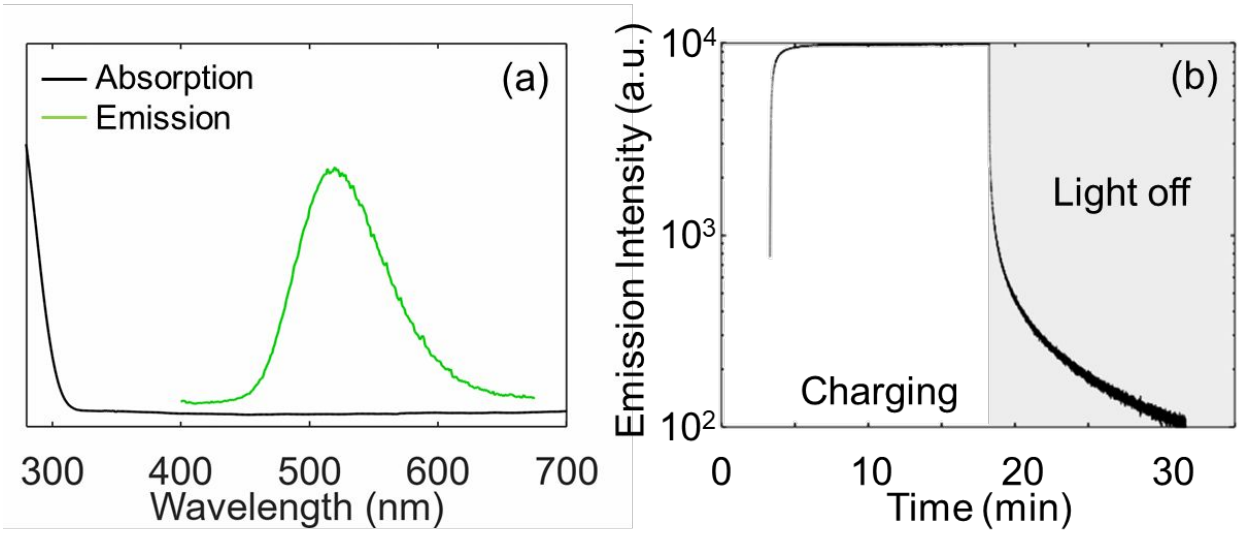

Figure 6. (a) Absorption and emission spectra and (b) luminescence kinetics for charging and discharging of $SrAl_2O_4$:Eu,Dy.

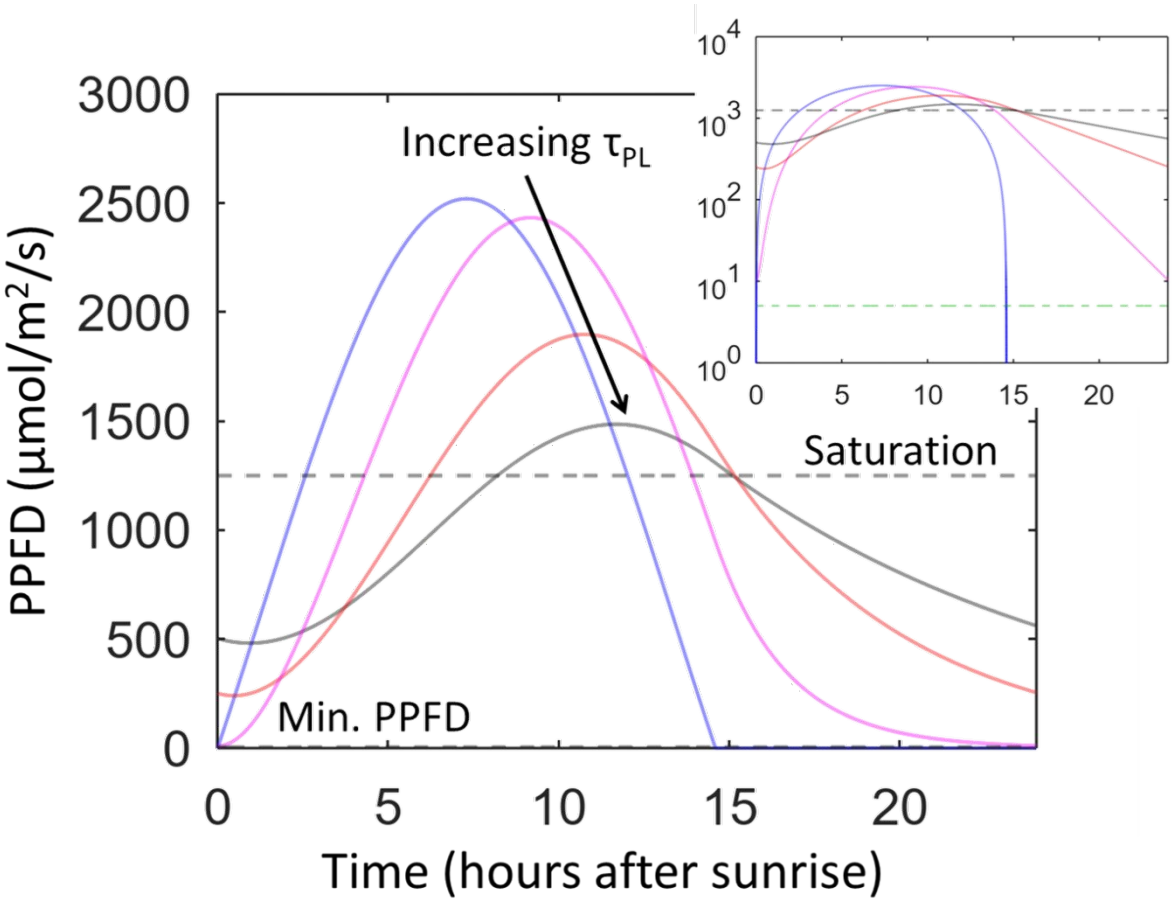

Figure 7. Shift in the distribution of available PAR (photosynthetically active radiation) photons throughout the day for a typical sun plant at Stanford University (and equivalent latitudes) as a result of fully down-converting UV and PAR wavelengths to PAR wavelengths with luminescent decay times of 2 hrs (magenta), 5.5 hrs (red), and 11 hrs (gray) with reference to regular sunlight (blue). Only photosynthetic photon flux densities (PPFD) between the minimum PPFD and light saturation lines (green and gray dotted lines, respectively) can be used to drive photosynthesis. The minimum PPFD line is more clearly visible on a log scale (see inset).

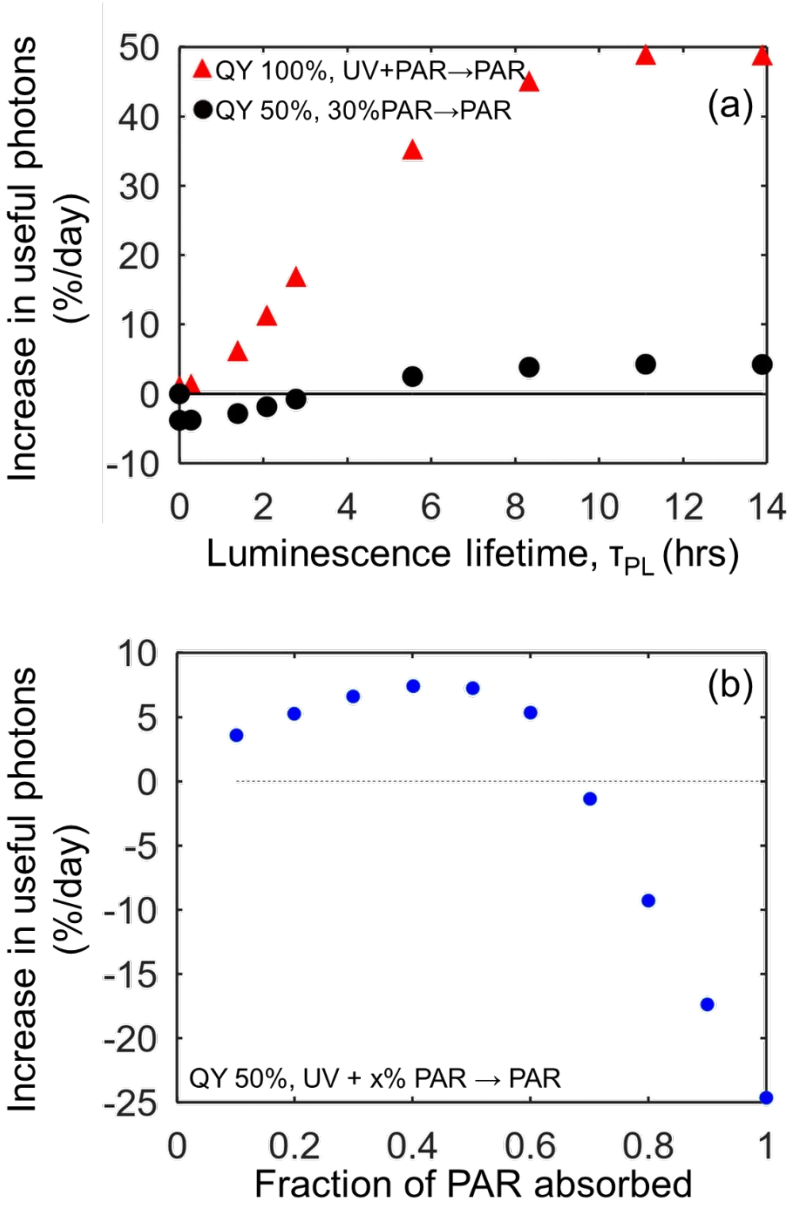

Figure 8. (a) Increase in cumulative number of photons between the minimum PPFD for photosynthesis and light saturation (for a sun plant) as a result of PersL of various characteristic decay times. Red points are for UV and visible light absorbed and reemitted as PAR with 100% quantum efficiency (encompassing both quantum yield and the efficiency with which emitted photons are captured by the plants) while black points are for 30% of PAR being absorbed and reemitted as PAR with 50% efficiency. Note that as of τ_{PersL}~2 hrs, plants no longer experience a fully dark night, free of any photosynthetic activity. (b) Trade-off in the integral useful photon count with increased absorption of PAR (and complete absorption of UV), assuming 50% quantum efficiency and a 14-hour lifetime: increasing PAR absorbed increases both the luminescent photon count and parasitic losses, resulting in an optimum.

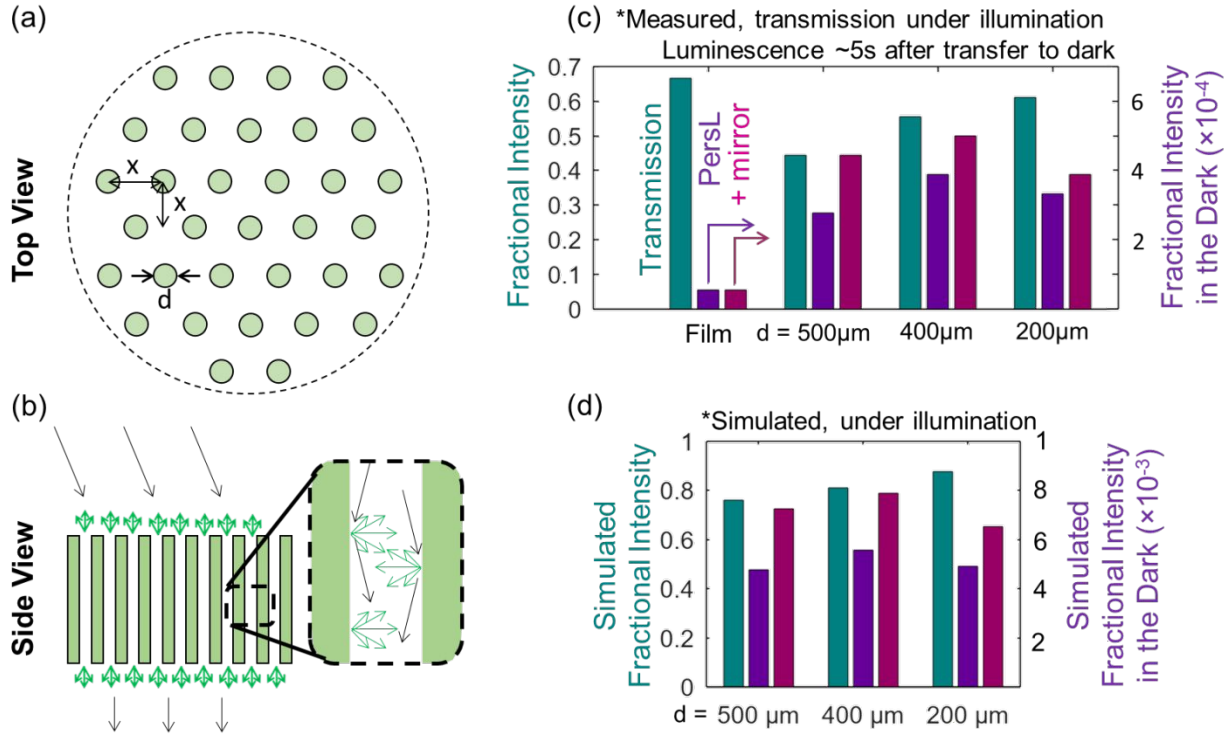

Figure 9. Schematic of the PersL concentrator, including (a) a top view and (b) a side view of the pillars of packed $SrAl_2O_4$:Eu,Dy embedded in a matrix of acrylic. Prototypes of this concentrator were made of thickness 6.4 mm, with x = 1.4 mm and various hole sizes, d = 500 μm, 400 μm, and 200 μm. The prototypes were charged with simulated solar light with a high PAR intensity of 1800 μmol/m^2/s. (c) Fractional intensity of light transmitted (left axis) and fractional intensity of downwards PersL without and with a reflective surface placed on the top (right axis) are benchmarked against a reference film of the same $SrAl_2O_4$:Eu,Dy (particles 50 – 75 μm) embedded in PMMA. Transmission was measured directly under illumination; in the luminescence measurement, a lag of ~5 s was introduced in transferring the device to the dark. The detection limit of the instrument used is 0.1 μmol/m^2/s. (d) Monte Carlo simulation results for the same geometries reported in panel (c), reported as the fractional intensity (relative to incoming irradiation) of transmission on the left axis and fraction intensity of luminescence without and with a top reflective surface on the right axis. The simulation treats a single point in time under illumination, meaning that the measured intensity in the dark, measured ~5 s after illumination, is expected to be about an order of magnitude lower in intensity.

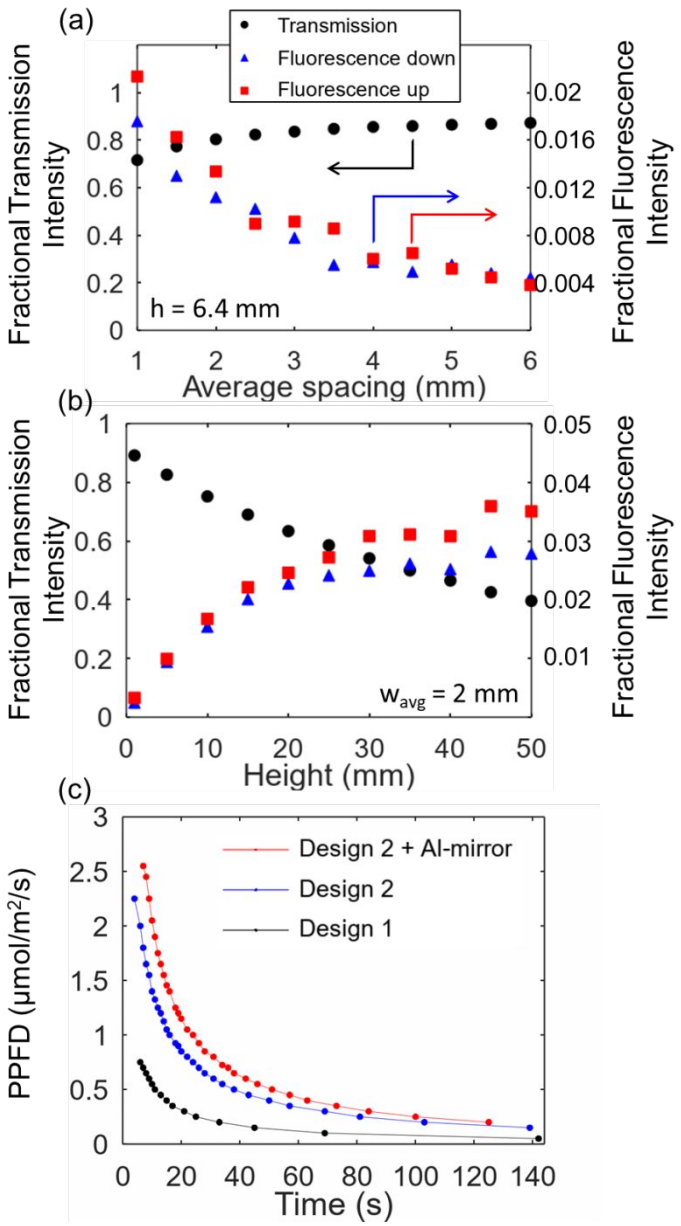

Figure 10. (a) Sensitivity analysis of the Monte Carlo simulation-derived transmission (left axis) and fluorescence up and down (right axis) to the angle-averaged spacing between columns of $SrAl_2O_4$:Eu,Dy, assuming a height of h = 6.4 mm and $SrAl_2O_4$:Eu,Dy column diameters of 200 μm. For reference, the value of x = 1.4 mm used in panels (c) and (d) corresponds to an angle-averaged spacing of 3.9 mm. (b) Sensitivity analysis of the Monte Carlo simulation-derived transmission (left axis) and fluorescence up and down (right axis) to the height of the concentrator, assuming an angle-averaged spacing between columns of w_{avg} = 2 mm and $SrAl_2O_4$:Eu,Dy column diameters of 200 μm. The same legend applies to panels (a) and (b). These simulation results were used as guidelines in designing an improved device (x = 0.8 mm, w_{avg} = 1.3 mm, d = 0.4 mm, h = 12.7 mm). (c) Measured luminescence kinetics of the improved device, "design 2," with and without a top, reflective (aluminum) surface, benchmarked against the "design 1" device (x = 1.4 mm, w_{avg} = 3.9 mm, d = 0.4 mm, h = 6.4 mm).

References

1 Grübler, A. (1998) *Technology and Global Change*. Cambridge Univ Press, Cambridge, UK.

2 DOE/SC-108. Carbon Cycling and Biosequestration. March 2008 Workshop.

3 Wolf, J.; West, T.O.; Page, Y.L.; Kyle, G.P.; Zhang, X.; Collatz, G.J.; Imhoff, M.L. (2015) Biogenic carbon fluxes from global agricultural production and consumption. *Global Biogeochem. Cycles,* 29, 1617-1639.

4 Mathew, I.; Shimelis, H.; Mutema, M.; Chaplot, V. (2017) What crop type for atmospheric carbon sequestration: Results from a global data analysis. *Agriculture, Ecosys., Env.*, 243, 34-46.

5 Xu, B.; Yang, Y.; Shen, H.; Fang, J. (2014) Global patterns of ecosystem carbon flux in forests: A biometric data-based synthesis. *Global Biogeochem. Cycles*, 28 (9), 962-973.

6 Foley, J. (2015) A Five-Step Plan to Feed the World. *National Geographic*. http://www.nationalgeographic.com/foodfeatures/feeding-9-billion/.

7 Bishopp, A., Lynch, J. (2015) The hidden half of crop yields. *Nature Plants* 1, 15117.

8 Zhu, X.-G.; Long, S.P.; Ort, D.R. (2010) Improving Photosynthetic Efficiency for Greater Yield. *Annual Rev. of Plant. Bio.* 61, 235-261.

9 Blankenship, R.E.; Tiede, D.M.; Barber, J.; Brudvig, G.W.; Fleming, G.; Ghirardi, M.; Gunner, M.R.; Junge, W.; Kramer, D.M.; Melis, A.; Moore, T.A.; Moser, C.C.; Nocera, D.G.; Nozik, A.J.; Ort, D.R.; Parson, W.W.; Prince, R.C.; Sayre, R.T. (2011) Comparing Photosynthetic and Photovoltaic Efficiencies and Recognizing the Potential for Improvement. *Science,* 332, 805-809.

10 Montgomery, D.R. (2007) Soil erosion and agricultural sustainability. *PNAS* 104 (33), 13268-13272.

11 World Bank, World Development Indicators. (2019). Agricultural land (% of land area) [Data file]. Retrieved from https://data.worldbank.org/indicator/AG.LND.AGRI.ZS?end=2016&start=1961

12 Pingali, P.L. (2012) Green Revolution: Impacts, limits, and the path ahead. *PNAS*, 109 (31), 12302-12308.

13 Gray, J.M.; Frolking, S.; Kort, E.A.; Ray, D.K.; Kucharik, C.J.; Ramankutty, N.; Friedl, M.A. (2014) Direct human influence on atmospheric CO_2 seasonality from increased cropland productivity. *Nature* 515, 398-401.

14 Kubis, A. and Bar-Even, A. (2019) Synthetic biology approaches for improving photosynthesis. *Journ. Experimental Botany*, 70 (5), 1425-1433.

15 Simkin, A.J.; López-Calcagno, P.E.; Raines, C.A. (2019) Feeding the world: improving photosynthetic efficiency for sustainable crop production. *J. Exp. Bot.* 70 (4), 1119-1140.

16 South, P.F.; Cavanagh, A.P.; Liu, H.W.; Ort, D.R. (2019) Synthetic glycolate metabolism pathways stimulate crop growth and productivity in the field. *Science* 363 (6422), eaat9077.

17 Song, Q.; Wang, Y.; Qu, M.; Ort, D.R.; Zhu, X.-G. (2017) The impact of modifying photosystem antenna size on canopy photosynthetic efficiency—Development of a new canopy photosynthesis model scaling from metabolism to canopy level processes. *Plant Cell Environ.* 40, 2946-2957.

18 Walker, B.J.; Drewry, D.T.; Slattery, R.A.; VanLoocke, A.; Cho, Y.B.; Ort, D.R. (2019) Chlorophyll Can Be Reduced in Crop Canopies with Little Penalty to Photosynthesis. *Plant Physiol.* 176, 1215-1232.

[19] Bolin, B. and Keeling, C.D. (1963) Large-Scale Atmospheric Mixing As Deduced from the Seasonal and Meridional Variations of Carbon Dioxide. *Journ. Geophys. Research*, 68 (13), 3899-3920.
[20] Adams, S.R. and Langton, F.A. (2005) Photoperiod and plant growth: a review. *The Journ. Of Hort. Sci. and Biotech.* 80 (1), 2-10.
[21] Hanan, J.J.; Holley, W.D.; Goldsberry, K.L. *Greenhouse Management*. Berlin: Springer-Verlag, 1978.
[22] Kozai, T.; Fujiwara, K.; Runkle, E.S. *LED Lighting for Urban Agriculture*. Singapore: Springer, 2016.
[23] Velez-Ramirez, A.I.; van Ieperen, W.; Vreugdenhil, D.; van Poppel, P.M.J.A.; Heuvelink, E.; Millenaar, F.F. (2014) A single locus confers tolerance to continuous light and allows substantial yield increase in tomato. *Nature Comm.* 5, 4549.
[24] Chen, M. and Blankenship, R.E. (2011) Expanding the solar spectrum used by photosynthesis. *Trends in Plant Sci.* 16 (8), 427-431.
[25] Mohsenpour, S.F.; Willoughby, N. (2013) Luminescent photobioreactor design for improved algal growth and photosynthetic pigment production through spectral conversion of light. *Bioresource Tech*., 142, 147-153.
[26] Jang, H.; Namgoong, J.W.; Sung, M.-G.; Chang, Y.; Kim, J.P. (2018) Synthesis and characterization of fluorescent dyes and their applications for the enhancement of growth rate of Chlorella vulgaris. *Dyes and Pigments*, 158, 142-150.
[27] Xia, Q.; Batentschuk, M.; Osvet, A.; Richter, P.; Häder, D.P.; Schneider, J.; Brabec, C.J.; Wondraczek, L.; Winnacker, A. (2013) Enhanced photosynthetic activity in Spinacia oleracea by spectral modification with a photoluminescent light converting material. *Opt. Express*, 21 (S6), A909-A916.
[28] Wondraczek, L.; Batentschuk, M.; Schmidt, M.A.; Borchardt, R.; Scheiner, S.; Seemann, B.; Schweizer, P.; Brabec, C. (2013) Solar spectral conversion for improving the photosynthetic activity in algae reactors. *Nature Comm.* 4, 1-6.
[29] UbiQD, Inc. UbiGro Ag Films and Greenhouses. https://ubiqd.com/agriculture/ (accessed Sep 5, 2019).
[30] Zhu, Y.; Anderson, D.B.; Jones, S.B. (2018) Algae Farm Cost Model: Considerations for Photobioreactors. PNNL-28201. Richland, WA: Pacific Northwest National Laboratory.
[31] Davis, R.; Markham, J.; Kinchin, C.; Grundl, N.; Tan, E.C.D.; Humbird, D. (2016). Process Design and Economics for the Production of Algal Biomass: Algal Biomass Production in Open Pond Systems and Processing Through Dewatering for Downstream Conversion. NREL/TP-5100-64772. Golden, CO: National Renewable Energy Laboratory.
[32] Huntley, M.E.; Johnson, Z.I.; Brown, S.L.; Sills, D.L.; Gerber, L.; Archibald, I.; Machesky, S.C.; Granados, J.; Beal, C.; Greene, C.H. (2015) Demonstrated large-scale production of marine microalgae for fuels and feed. *Algal Research* 10, 249-265.
[33] Beal, C.M.; Gerber, L.N.; Sills, D.L.; Huntley, M.E.; Machesky, S.C.; Walsh, M.J.; Tester, J.W.; Archibald, I.; Granados, J.; Greene, C.H. (2015) Algal biofuel production for fuels and feed in a 100-ha facility: A comprehensive techno-economic analysis and life cycle assessment. *Algal Research* 10, 266-279.
[34] Inada, K. (1976) Action spectra for photosynthesis in higher plants. *Plant Cell Physiol.* 17, 355-365.
[35] Gates, D.M.; Keegan, H.J.; Schleter, J.C.; Weidner, V.R. (1965) Spectral Properties of Plants. *Appl. Optics*, 4, 11-20.

[36] Balegh, S. E. and Bidulph, O. (1970) The Photosynthetic Action Spectrum of the Bean Plant. *Plant Physiol.*, 46, 1-5.

[37] McCree, K. J. (1971-1972) The action spectrum, absorptance and quantum yield of photosynthesis in crop plants. *Agricultural Meteorology*, 9, 191-216.

[38] Nishio, J.N. (2000) Why are higher plants green? Evolution of the higher plant photosynthetic pigment complement. *Plant, Cell and Env.* 23, 539-548.

[39] Terashima, I.; Fujita, T.; Inoue, T.; Chow, W.S.; Oguchi, R. (2009) Green Light Drives Photosynthesis More Efficiently than Red Light in Strong White Light: Revisiting the Enigmatic Question of Why Leaves are Green. *Plant Cell Physiol.* 50 (4), 684-697.

[40] Slattery, R.A.; Grennan, A.K.; Sivaguru, M.; Sozzani, R.; Ort, D.R. (2016) Light sheet microscopy reveals more gradual light attenuation in light-green versus dark-green soybean leaves. *J. Exp. Bot.* 67 (15), 4697-4709.

[41] Sun, J.; Nishio, J.N.; Vogelmann, T.C. (1998) Green Light Drives CO_2 Fixation Deep within Leaves. *Plant Cell Physiol*. 39 (10), 1020-1026.

[42] Cui, M.; Vogelmann, T.C.; Smith, W.K. (1991) Chlorophyll and light gradients in sun and shade leaves of *Spinacia oleracea*. *Plant, Cell and Env.* 14, 493-500.

[43] Terashima, I. and Saeki, T. (1985) A New Model for Leaf Photosynthesis Incorporating the Gradients of Light Environment and of Photosynthetic Properties of Chloroplasts within a Leaf. *Annals of Botany*, 56 (4), 489-499.

[44] Vogelmann, T. C. and Martin, G. (1993) The functional significance of palisade tissue: penetration of directional versus diffuse light. *Plant, Cell & Env.*, 16, 65-72.

[45] Long, S.P.; Zhu, X.-G.; Naidu, S.L.; Ort, D.R. (2006) Can improvement in photosynthesis increase crop yields? *Plant Cell Environ.* 29 (3), 315-330.

[46] Zhou, Y.; Schideman, L.C.; Park, D.S.; Stirbet, A.; Govindjee; Rupassara, S.I.; Krehbiel, J.D.; Seufferheld, M.J. (2015) Characterization of a Chlamydomonas reinhardtii mutant strain with improved biomass production under low light and mixotrophic conditions. *Algal Research* 11, 134-147.

[47] Bonente, G.; Pippa, S.; Castellano, S.; Bassi, R.; Ballottari, M. (2012) Acclimation of Chlamydomonas reinhardtii to Different Growth Irradiances. *J. Biol. Chem.* 287 (8), 5833-5847.

[48] Strenkert, D.; Schmollinger, S.; Gallaher, S.D.; Salomé, P.A.; Purvine, S.O.; Nicora, C.D.; Mettler-Altmann, T.; Soubeyrand, E.; Weber, A.P.M.; Lipton, M.S.; Basset, G.J.; Merchant, S.S. (2019) Multiomics resolution of molecular events during a day in the life of Chlamydomonas. *PNAS* 116 (6), 2374-2383.

[49] Folta, K.M. and Maruhnich, S.A. (2007) Green light: a signal to slow down or stop. *J. Exp. Bot.* 58 (12), 3099-3111.

[50] Wang, Y. and Folta, K.M. (2013) Contributions of green light to plant growth and development. *Am. J. Bot.* 100, 70-78.

[51] Dougher, T.A. and Bugbee, B. (2001) Evidence for yellow light suppression of lettuce growth. *Photochem. Photobiol.* 73 (2), 208-212.

[52] Zhou, Y. and Singh, B.R. (2002) Red light stimulates flowering and anthocyanin biosynthesis in American cranberry. *Plant Growth Regulation*, 38, 165-171.

[53] Taniguchi, M. and Lindsey, J.S. (2017) Database of Absorption and Fluroescence Spectra of >300 Common Compounds for use in PhotochemCAD. *Photochemistry and Photobiology*, 94, 290-327.

[54] Ruedas-Rama, M.J.; Walters, J.D.; Orte, A.; Hall, E.A.H. (2012) Fluorescent nanoparticles for intracellular sensing: a review. *Analytica Chimica Acta*, 751, 1-23.

[55] Resch-Genger, U.; Grabolle, M.; Cavaliere-Jaricot, S.; Nitschke, R.; Nann, T. (2008) Quantum dots versus organic dyes as fluroescent labels. *Nature Methods*, 5, 763-775.

[56] Xu, G.; Zeng, S. ; Zhang, B.; Swihart, M.T.; Yong, K.-T.; Prasad, P.N. (2016) New generation cadmium-free quantum dots for biophotonics and nanomedicine. *Chem. Rev.*, 116, 12234-12327.

[57] Pang, L.; Shen, Y.; Tetz, K.; Fainman, Y. (2005) PMMA quantum dots composites fabricated via use of pre-polymerization. *Opt. Express*, 13 (1), 44-49.

[58] Slattery, R.A.; Walker, B.J.; Weber, A.P.M.; Ort, D.R. (2018) The impacts of fluctuating light on crop performance. *Plant Physiol.*, 176, 990-1003.

[59] Kromdijk, J.; Glowacka, K.; Leonelli, L.; Gabilly, S.T.; Iwai, M.; Niyogi, K.K.; Long, S.P. (2016) Improving photosynthesis and crop productivity by accelerating recovery from photoprotection. *Science* 354 (6314), 857-861.

[60] Taylor, S.H. and Long, S.P. (2017) Slow induction of photosynthesis on shade to sun transitions in wheat may cost at least 21% of productivity. *Phil. Trans. R. Soc. B*. 372, 20160543.

[61] Xu, J. and Tanabe, S. (2019) Persistent luminescence instead of phosphorescence: History, mechanism, and perspective. *J. Lumin.* 205, 581-620.

[62] Dutczak, D.; Jüstel, T.; Ronda, C.; Meijerink, A. (2015) Eu^{2+} luminescence in strontium aluminates. *Phys. Chem. Chem. Phys.* 17, 15236-15249.

[63] Botterman, J.; Joos, J.J.; Smet, P.F. (2014) Trappping and detrapping in $SrAl_2O_4$:Eu,Dy persistent phosphors: Influence of excitation wavelength and temperature. *Phys. Rev. B* 90, 085147.

[64] Smets, B.; Rutten, J.; Hoeks, G.; Verlijsdonk, J. (1989) $2SrO \cdot 3Al_2O_3:Eu^{2+}$ and $1.29(Ba,Ca)O,6Al_2O_3:Eu^{2+}$: Two New Blue-Emitting Phosphors. *J. Electrochem. Soc.* 136 (7), 2119-2123.

[65] Van der Heggen, D.; Joos, J.J.; Smet, P.F. (2018) Importance of Evaluating the Intensity Dependency of the Quantum Efficiency: Impact on LEDs and Persistent Phosphors. *ACS Photonics* 5, 4529-4537.

[66] Katsumata, T.; Sasajima, K.; Nabae, T.; Komuro, S.; Morikawa, T. (1998) Characteristics of Strontium Aluminate Crystals Used for Long-Duration Phosphors. *J. Am. Ceram. Soc.* 81 (2), 413-416.

[67] Rojas-Hernandez, R.E.; Rubio-Marcos, R.; Rodriguez, M.A.; Fernandez, J.F. (2018) Long lasting phosphors : SrAl2O4 :Eu,Dy as the most studied material. *Renew. Sust. Energy Reviews*, 81 (2), 2759-2770.

[68] Kabe, R. and Adachi, C. (2017) Organic long persistent luminescence. *Nature* 550, 384-387.

[69] Jinnai, K.; Kabe, R.; Adachi, C. (2018) Wide-Range Tuning and Enhancement of Organic Long-Persistent Luminescence Using Emitter Dopants. *Adv. Mater.* 30, 1800365.

[70] Ubiquitous Energy, Inc. (2019, March 20) Ubiquitous Energy Certifies New World Record Performance for Transparent Solar Cell [Press release]. Retrieved from https://www.businesswire.com/news/home/20190320005019/en/Ubiquitous-Energy-Certifies-New-World-Record-Performance/

[71] Zhang, K.Y.; Yu, Q.; Wei, H.; Liu, S.; Zhao, Q.; Huang, W. (2018) Long-Lived Emissive Probes for Time-Resolved Photoluminescence Bioimaging and Biosensing. *Chem. Rev.* 118 (4), 1770-1839.

[72] Allorent, G. ; Lefebvre-Legendre, L. ; Chappuis, R. ; Kuntz, M. ; Truong, T.B. ; Niyogi, K.K.; Ulm, R.; Goldschmidt-Clermont, M. (2016) UV-B photoreceptor-mediated protection of the photosynthetic machinery in *Chlamydomonas reinhardtii*. *PNAS*, 113 (51), 14864-14869.

[73] Vitola, V.; Millers, D.; Bite, I.; Smits, K.; Spustaka, A. (2019) Recent progress in understanding the persistent luminescence in SrAl2O4:Eu,Dy. *Materials Science and Technology* 35 (14), 1661-1677.

[74] Botterman, J.; Joos, J.J.; Smet, P.F. (2014) Trapping and detrapping in SrAl2O4:Eu,Dy persistent phosphors: Influence of excitation wavelength and temperature. *Phys. Rev. B*, 90, 085147.

[75] Botterman, J. and Smet, P.F. (2015) Persistent phosphor SrAl2O4:Eu,Dy in outdoor conditions: saved by the trap distribution. *Opt. Express*, 23 (15), A868-A881.

[76] Nakanishi, T. (2015) Preparation of europium-activated SrAl2O4 glass composites using the frozen sorbet technique. *J. Ceramic Soc. Japan*, 123 (9), 862-867.

[77] Tanaka, T. (1979) Optical Constants of Polycrystalline 3d Transition Metal Oxides in the Wavelength Range 350 to 1200 nm. *Jpn. J. Appl. Phys.*, 18 (6), 1043-1047.